OPEN

Nickel-cobalt bimetallic anode catalysts for direct urea fuel cell

Wei Xu, Huimin Zhang, Gang Li & Zucheng Wu

Department of Environmental Engineering, Laboratory of Electrochemistry and Energy Storage; State Key laboratory of Clean Energy Utilization, Zhejiang University, Hangzhou 310058, P. R. China.

Nickel is an ideal non-noble metal anode catalyst for direct urea fuel cell (DUFC) due to its high activity. However, there exists a large overpotential toward urea electrooxidation. Herein, NiCo/C bimetallic nanoparticles were prepared with various Co contents (0, 10, 20, 30 and 40 wt%) to improve the activity. The best Co ratio was 10% in the aspect of cell performance, with a maximum power density of 1.57 mW cm^{-2} when 0.33 M urea was used as fuel, O_2 as oxidant at 60°C. The effects of temperature and urea concentration on DUFC performance were investigated. Besides, direct urine fuel cell reaches a maximum power density of 0.19 mW cm^{-2} with an open circuit voltage of 0.38 V at 60°C.

U rea, widely used as fertilizer, can be produced via series chemical processes by using H_2, N_2 and CO_2[1,2]. It is an ideal H_2 and CO_2 storage medium due to its high energy density (16.9 MJ L^{-1}, 10.1 weight percent of H_2), safety and convenience of transportation[3,4]. Figure 1 demonstrates that urea functions as an important intermediate in a nitrogen and carbon recycle system. N_2 and CO_2 can be achieved from air, and H_2 can be produced from water. NH_3, synthesized from H_2 and N_2, has been proposed as an alternative hydrogen storage material with high H density. Although in wide use, ammonia is both caustic and hazardous. When combined with CO_2, a much safer precursor of ammonia – urea is formed, and the carbon dioxide is fixed at the same time. As energy medium, a critical factor is to release hydrogen for controlled delivery to presumably energy producing device. In this case, hydrogen is normally released thermally or through the use of hydrolysis or metal catalyst. There is also the possibility of directly retrieving energy from urea via direct urea fuel cell (DUFC) with high efficiency to complete the carbon and nitrogen recycle in figure 1. Besides, another main urea source is naturally the urea or urine rich wastewater, which is often leading to eutrophication[5,6]. Those urea/urine wastewaters can possibly be treated through oxidation reaction in DUFC to release nitrogen gas before their discharge into environments, or even turned to recycle water after further treatment.

DUFC is one of the key points to utilize urea in figure 1. In DUFC system, anode catalyst is a crucial component to catalyze urea oxidation reaction (UOR). Usually, noble metals such as Pt, Pd and multi-metal catalysts based on them are used as anode catalysts in fuel cells with high activity[7-11]. However, noble metals will greatly increase the fuel cells cost and low activities toward UOR are observed in experiments[12]. Nickel, an inexpensive metal, shows high activity and stability, thus it is often attempted to adopt as anode catalyst in DUFC. Note that a large overpotential was reported (ca. 0.45 V vs. SHE), compared to the theoretical potential of UOR (-0.46 V vs. SHE)[13]. It is reasonable that if we can reduce the overpotential, a better DUFC performance might be achieved.

Interestingly, cobalt was widely used as additive to form bimetal catalysts such as NiCo, PtCo and PdCo[14-17] to improve electro-activity of catalysts due to the particular electronic property of the bimetals. Among them, nickel-cobalt bimetal has been intensively developed as efficient anode catalyst toward electrocatalytic oxidation of urea[18-20]. Instead of power input for anodic oxidation, bimetallic catalysts could be a good choice for fuel cell[17]. Herein, it is feasible to apply nickel-cobalt bimetal for anode catalyst in DUFC to directly produce electricity. However, some researches drew opposite conclusions. Results demonstrated that the addition of Co could decrease the current densities of anodic peaks and even result in positive shifts of electro-oxidation onset potential[21-23]. It is believed that the Co contents and preparation methods are responsible for the different results of catalysts activities toward oxidation reactions. Accordingly, it is important to deeply survey the effect of Co addition on other metals. In this work, we focus on carbon supported Ni-Co bimetal catalyst aiming to enhance the activity toward UOR, and further improve the performance of DUFC. Herein, NiCo/C catalysts are prepared via NaBH$_4$ reduction method with different Co contents, and they are used as anode catalyst in DUFC to examine the activity. Besides, human urine, containing about 9.3 g L^{-1} urea[24], was possibly used as fuel in DUFC for its applicability study. Given the urea density of 1.335 g mL^{-1}, the energy density of urine is 118 kJ L^{-1}. It is a large
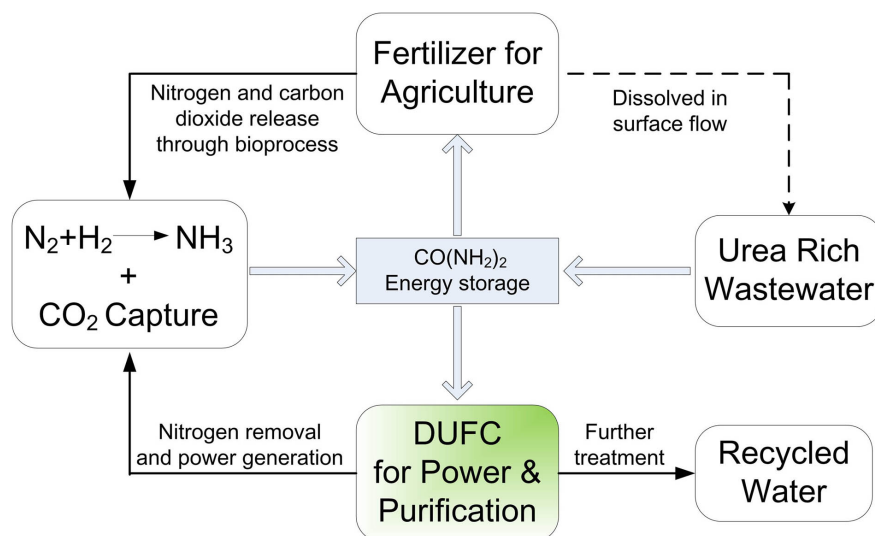
Figure 1 | Schematic of nitrogen and carbon dioxide recycle with urea as intermediate.

amount of energy considering the huge population of humans and animals all over the world. Thus we also test the cell performance using urine as fuel with NiCo/C catalyst.

Results

SEM and TEM analyses were made in order to get information on the particle size and uniformity. Fig. 2(a) and (b) show the SEM images of Ni/C (50 wt% Ni) and NiCo/C (10 wt% Co, 40 wt% Ni) respectively. The amount of Ni and Co supported on carbon black was roughly calculated by weighing $NiSO_4$ and $CoCl_2$ before the reduction process. In the SEM images, numerous Ni or NiCo particles were uniformly distributed on carbon though some agglomerations were observed. The secondary particle size of the prepared Ni/C is about several 10^{-1} μm. Similarly, the NiCo/C has secondary particle size of $0.2 \sim 1$ μm, having a large specific area. TEM image of Ni/C particle is shown in fig. 2(c). Ni/C nanospheres with primary particle size of ~40 nm were prepared by $NaBH_4$ reduction. Ni/C nanoparticles were homogeneously and densely dispersed over the surface of carbon black. Fig. 2(d) demonstrates that most NiCo/C nanoparticles have primary particle size of 30 to 40 nm, though some much smaller particles with particle size of ~5 nm were observed. It is supposed that the particle size of the catalysts were depended on the reduction condition (i.e. solution and $NaBH_4$ concentration, the speed of adding $NaBH_4$, temperature, pH).

XRD patterns of Ni/C and NiCo/C were demonstrated in fig. 2(e). The blue line was the Ni/C XRD pattern. There is a strongest diffraction at $2\theta \sim 45°$ identified to be Ni (101) peak, indicating the formation of nickel. The peaks at $2\theta \sim 60°$ and ~71° signify nickel particle having a hexagonal structure. A nickel hydroxide peak is also observed at 2θ near 34°, revealing that some nickel was prepared in the form of $Ni(OH)_2$. When cobalt was added (red line), the Ni (101) peak became much smaller, almost disappeared from the NiCo/C pattern. On the contrary, the nickel hydroxide peak became larger at $2\theta \sim 34°$. It indicated that the incorporation of Co would promote much more nickel changing into the form of nickel hydroxide. Co (111) peak and $Co(OH)_2$ peak were detected at $2\theta \sim 44°$ and ~55° respectively, indicating the formation of NiCo/C catalyst. The peaks at $2\theta \sim 24°$ observed in both Ni/C and NiCo/C patterns were attributed to carbon black.

The surface composition of NiCo/C was further confirmed by XPS measurement, and the results were shown in figs. 2(f) and 2(g). In fig. 2(f), metallic Ni of $Ni_{2p1/2}$ and $Ni_{2p3/2}$ were detected at 870.2 eV and 852.8 eV, respectively. In the $Ni_{2p3/2}$ spectrum, NiO peak appeared at 853.7 eV. The peaks of 854.9 eV, 857.7 eV and

858.9 eV are ascribed to the $Ni(OH)_2$ peak, β-NiOOH peak and the Ni electron energy-loss peak, respectively[25,26]. The $Ni(OH)_2$ and β-NiOOH together account for about 29.4% of the total Ni element on the surface, a result from XPS peak area. It has also been found that metallic Co and $Co(OH)_2$ were on the surface of NiCo/C from the Co_{2p} XPS spectra in fig. 2(g). The main peaks at 778.1 eV and 794.0 eV were attributed to the metallic Co of $Co_{2p3/2}$ and $Co_{2p1/2}$. The $Co_{2p3/2}$ spectrum contains a $Co(OH)_2$ peak at 780.4 eV. The Co element constituted about 26.6% of the total Ni and Co elements on the surface.

It is expected that the addition of Co would enhance the Ni activity toward UOR, thus improve DUFC performance. Fig. 2(h) demonstrated the DUFC performance using Ni/C (Cell A) or NiCo/C (Cell B) as anode catalyst. Both cells used 0.33 M urea as fuels and humidification oxygen as electrons acceptor. Cell A achieved a maximum power density (P_{max}) of 1.4 mW cm^{-2} with an open circuit voltage (OCV) of 0.57 V. In comparison with Cell A, Cell B achieved a larger maximum power density of 2.0 mW cm^{-2} with an OCV of 0.64 V. The P_{max} of Cell B was 1.43 times that of Cell A. Besides, a more significant decline of cell voltage was observed in Cell A, which was attributed to the electrochemical polarization. It indicated that the NiCo/C catalyst with 10 wt% Co content could perform better than the Ni/C catalyst.

Discussion

XRD and XPS measurements demonstrated that nickel hydroxide was synthesized when the Co was incorporated. The increased nickel hydroxide will lead to the more active sites exposed for UOR[27-29], possibly one reason for DUFC improvement. In order to further explain the reason why the addition of cobalt would influence the catalytic activity, CVs of 0.33 M urea in 1 M KOH were tested. All the catalysts have the same metal weight percent of 50% in order to compare the catalysts activity under the same metallic content, i.e. NiCo or Ni were mixed with carbon at a 5/5 mass ratio. The subscripts of Ni and Co represent the mass ratio of Ni/Co. Fig. 3(a) shows a pair of reduction and oxidation peaks between 0.25 to 0.55 V vs. MMO. These peaks are regarded as the reversible conversion of $Ni(OH)_2$ (Ni^{2+}) $\leftrightarrow$ NiOOH (Ni^{3+}) in alkaline system[19]. A significant increase on current with the onset potential ca. 0.44 V vs. MMO was revealed when urea was added. The onset potential of UOR is the same as the potential where NiOOH (Ni^{3+}) is formed. This phenomenon demonstrates that urea is possibly electro-oxidized on catalytic NiOOH (Ni^{3+}). Thus, it is reasonable that the onset potential of UOR will decrease if we can generate NiOOH (Ni^{3+}) at a

2
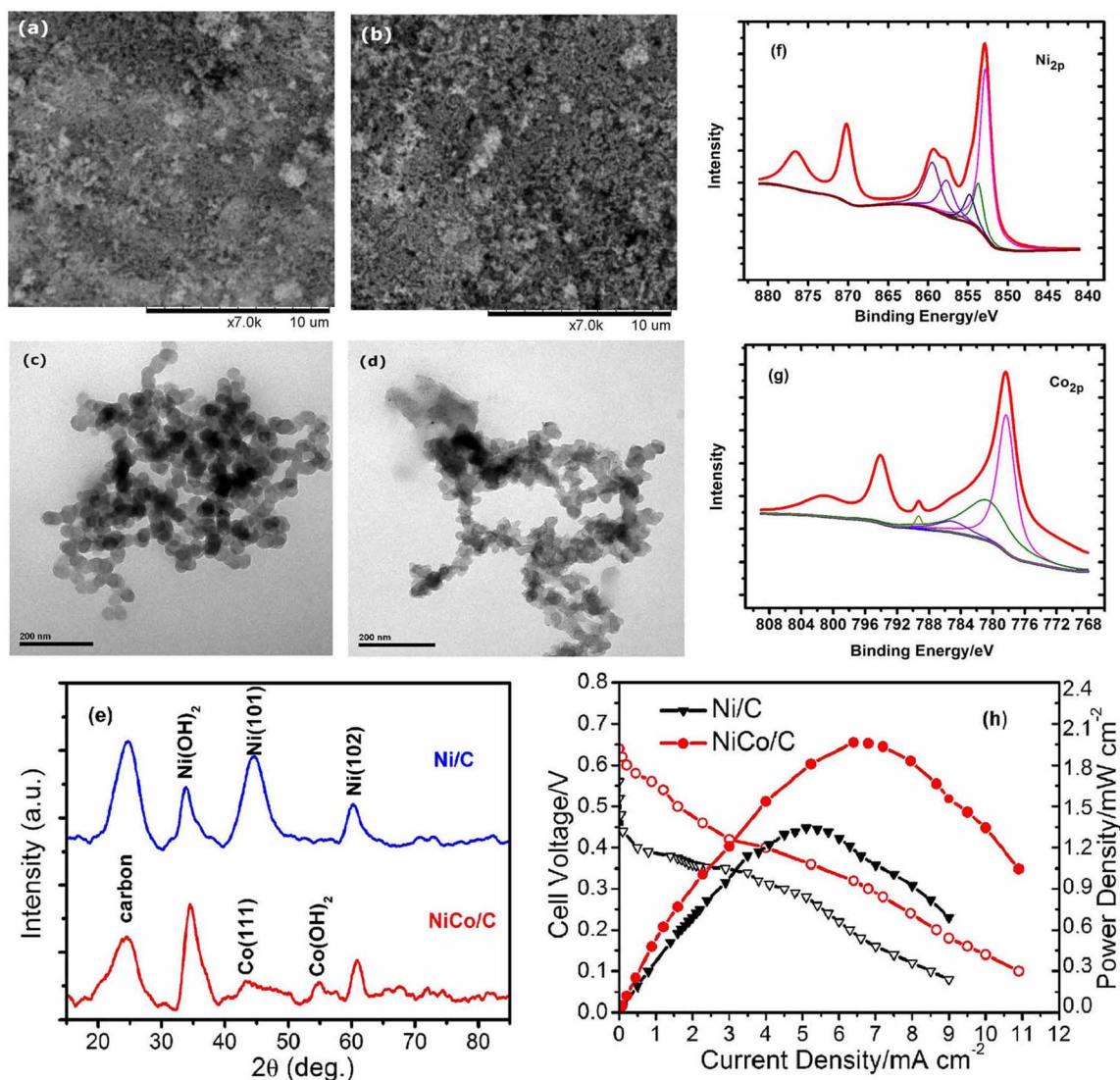
Figure 2 | Characterizations of catalysts and DUFC performance. SEM images of (a) Ni/C and (b) NiCo/C. TEM images of (c) Ni/C and (d) NiCo/C. (e) XRD patterns of Ni/C (blue) and NiCo/C (red). XPS spectra of NiCo/C for (f) Ni_{2p} and (g) Co_{2p}. (h) Polarization and power density curves of DUFC at 60°C with 0.33 M urea as fuel and humidification oxygen as electrons acceptor using Ni/C or NiCo/C as anode catalyst, Pt/C as cathode catalyst.

smaller potential. Fig. 3(b) demonstrates the onset potential of UOR shifts left to ca. 0.38 V *vs*. MMO, showing a decline of 60 mV in the overpotential of UOR. According to above discussion, the decline of UOR onset potential is due to the smaller potential where NiOOH (Ni^{3+}) is formed. As a preferable overpotential is observed in CV tests, the Ni_4Co_1/C catalyst may improve the electrochemical polarization in DUFC, which is in accordance with the results in fig. 2(h). If the Co content is increased, forming Ni_3Co_2/C in fig. 3(c), the onset potential decreases further to ca. 0.31 V *vs*. MMO, 130 mV less compared to Ni/C. It can be explained that Ni reaches a higher oxidation state during the UOR and promotes the electrons transfer when Co is doped[30,31]. This property can be confirmed by electrical conductivity (σ) tests at 20°C. Fig. (3f) shows that the electrical conductivity of Ni/C is ~0.131 S cm^{-1}. It increases as the amount of Co addition, reaching ~0.168 S cm^{-1} of Ni_4Co_1/C and ~0.201 S cm^{-1} of Ni_3Co_2/C, respectively. This phenomenon is in accordance with catalytic activity improvement of NiCo/C bimetal catalysts. However, as the Co contents continue to increase, although the σ still becomes larger, the onset potential will shift to positive direction. The onset potential of Ni_2Co_3/C is 0.38 V vs. MMO shown in fig. 3(d) and it shifts to 0.41 V when using Ni_1Co_4/C as catalyst shown in fig. 3(e). The onset potentials using NiCo/C catalysts are

summarized in fig. 3(f). Briefly, the incorporation of Co will reduce the onset potential, and the most negative one is achieved when using Ni_3Co_2/C. Further increase the Co content will lead to larger onset potential. Besides, the electro-oxidation current of urea is decreasing as the Co content in NiCo/C increasing. The main reason may be that cobalt is inactive for UOR, which decreases the exposed nickel active sites, thus hinder the UOR[19]. The addition of Co had advantages (reducing onset potential, ROP) as well as disadvantages (reducing electro-oxidation potential, REP), so it is important to seek a balance between the two effects in order to achieve the best catalyst activity. Based on this, we suppose the DUFC performance is depended on the positive influence of ROP and negative influence of REP.

The activity of NiCo/C toward UOR is further evaluated in DUFC. Fig. 4(a) shows the DUFC has the largest electricity output when using NiCo/C catalyst with 10% Co. The cell performance will decline when the Co contents exceeded 10%. Although the most negative onset potential in CV tests was achieved when using Ni_3Co_2/C catalyst, the optimal P_{max} of DUFC was observed using Ni_4Co_1/C as anode catalyst. That was because the electro-oxidation current in CVs dropped rapidly when the Co content exceeded 10% due to the Co inactivation toward UOR. The negative influence of REP was larger than positive influence of ROP. Fig. 4(b) outlined the
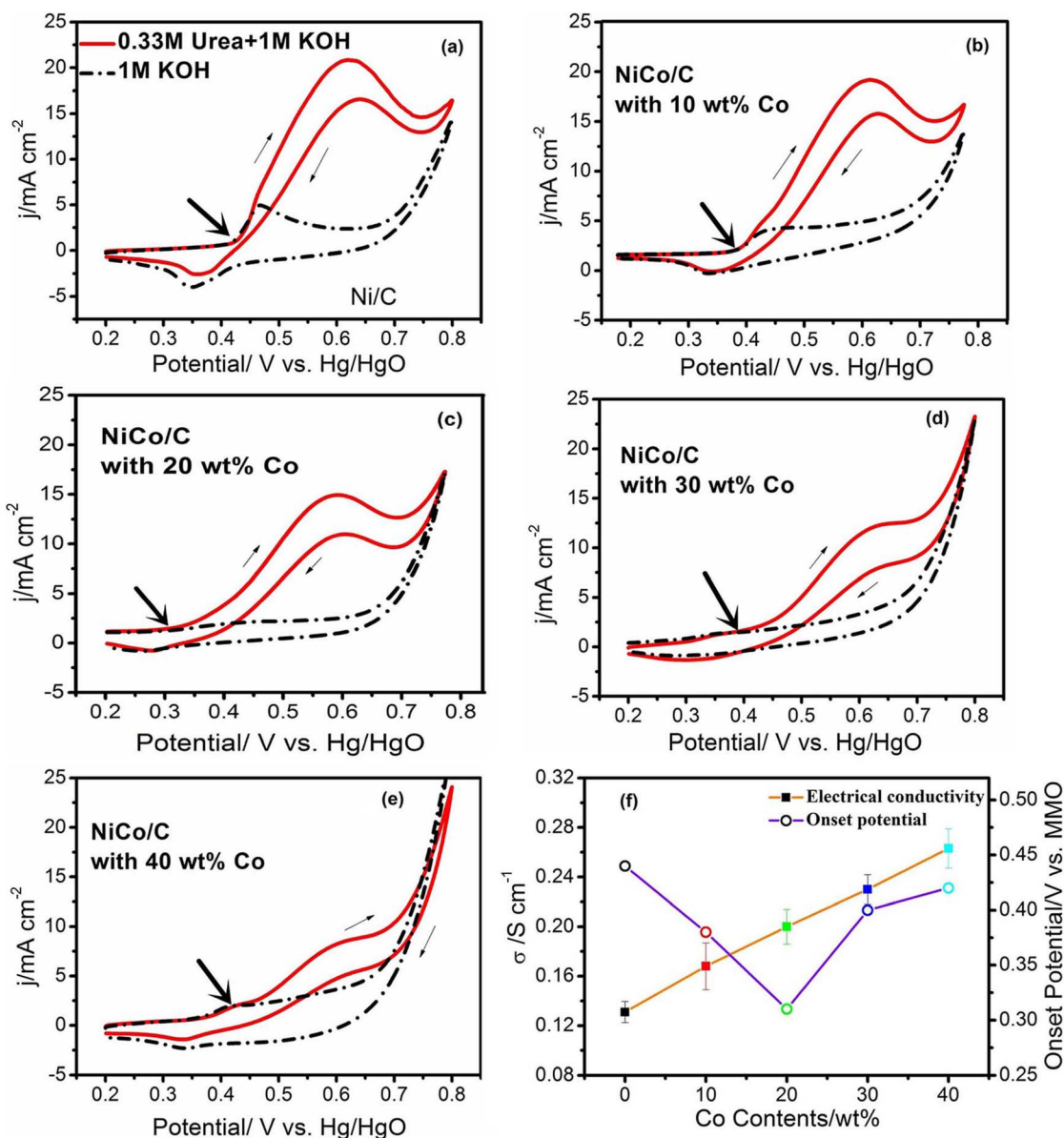
Figure 3 | Cyclic voltammograms (CVs). The Cvs were measured in 1 M KOH or 0.33 M urea + 1 M KOH at 20°C. The CVs were conducted on (a) Ni/C, (b) Ni_4Co_1/C, (c) Ni_3Co_2/C, (d) Ni_2Co_3/C and (e) Ni_1Co_4/C coated GCE at a scan rate of 50 mV s^{-1}. (f) Electrical conductivity of samples (data are an average of three runs; error bars indicate the standard deviation) and summary of onset potentials.

OCV and P_{max} of DUFC using NiCo/C as anode catalyst with various Co contents. The P_{max} continued to decrease as Co content increasing from 20% to 40%. Results showed the P_{max} of Ni_2Co_3/C was similar to that of Ni/C, and the P_{max} of Ni_1Co_4/C was a little smaller than that of Ni/C. This was reasonable because the UOR over-potential turned to became larger after Co content exceeding 20%, and thus the positive influence of ROP got smaller, even disappeared. However the negative influence of REP would still become larger, thus doping too much of Co would not have better effect on the P_{max} of DUFC. Note that the highest OCV of DUFC was achieved when using Ni_3Co_2/C as anode catalyst. This was in accordance with the ROP effect in CV tests, indicating that a smaller over-potential was to the benefit of a higher OCV due to the less polarisation loss.

Higher temperature is beneficial to the catalytic activity of NiCo/C, and it will enhance the reaction kinetics of urea hydrolysis and UOR. Fig 4(c) shows the maximum power density decrease to 1.6 mW cm^{-2} at 40°C and 1.4 mW cm^{-2} at 20°C, respectively. Higher drop in voltage with current density is found at lower voltage

(after 0.4 V) at 20°C and 40°C than that at 60°C, indicating the lower concentration or diffusion resistance at high temperature. However, ammonia gas will be generated significantly at high temperature (above 60°C) due to the urea hydrolysis. This will cause the fuels loss and gas leakage.

Fig. 4(d) shows the DUFC performance using human urine as fuels with NiCo/C anode catalyst. A maximum power density of 0.06 mW cm^{-2} is achieved with an OCV of 0.3 V at 20°C. Higher temperature will improve the cell performance owing to the better catalytic activity of the electrode and reaction kinetics. The maximum power density increases to 0.08 mW cm^{-2} at 40°C and 0.2 mW cm^{-2} at 60°C, when the urine sample containing about 0.1 M urea was applied. Compared to the fuel cell using 0.1 M urea as fuel (with an OCV of 0.45 V and a maximum power density of ~0.3 mW cm^{-2}), the cell performance of urine fuel cell (with an OCV of 0.38 V and a maximum power density of ~0.2 mW cm^{-2}) was insignificantly different at 60°C. Urine is a main contaminant in the municipal wastewater, and it is also an ideal energy resource
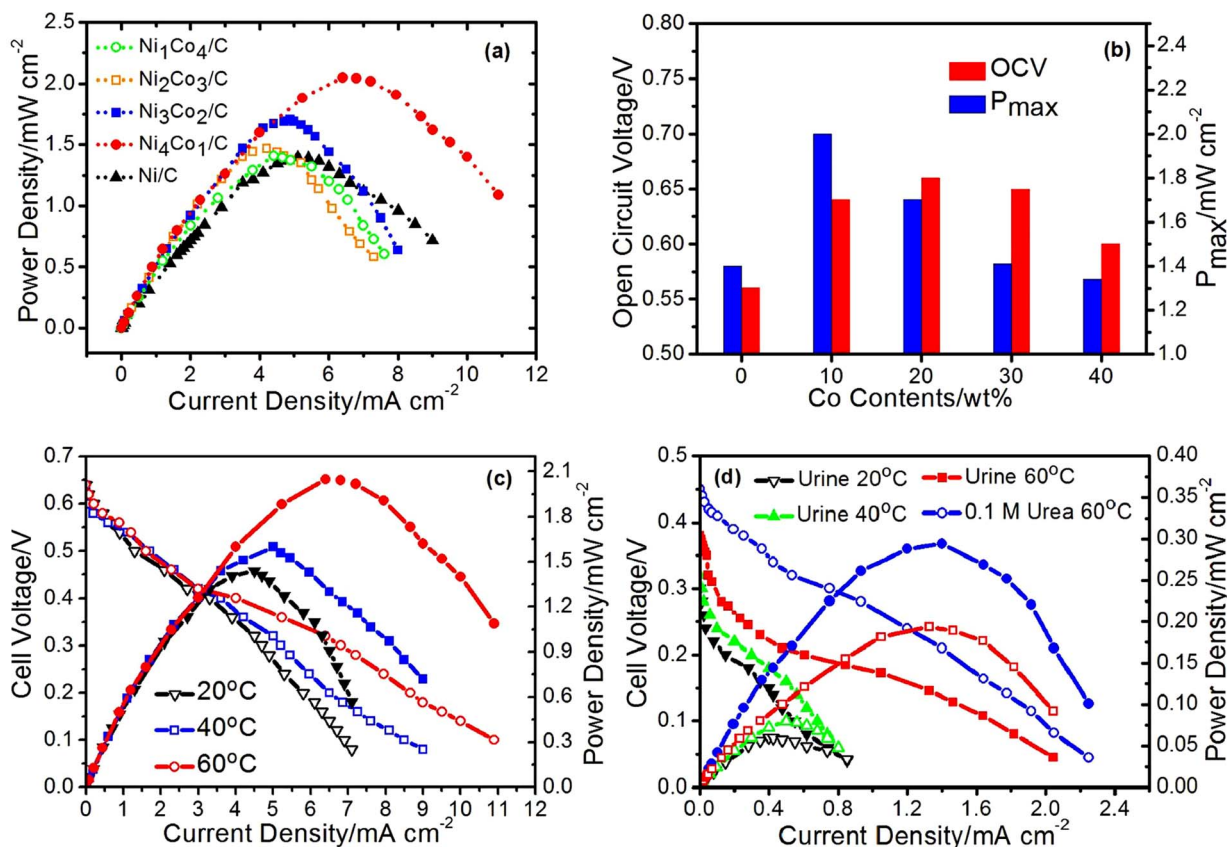
Figure 4 | DUFC performance. (a) Power density curves of DUFC using NiCo/C catalysts with different Co contents. (b) The effects of catalysts on DUFC maximum power density and open circuit voltage. (c) DUFC performance using 0.33 M urea at 20, 40, 60°C with Ni_4Co_1/C as anode catalyst and (d) Human urine was used as fuel in DUFC at 20°C, 40°C and 60°C, respectively, in comparison with 0.1 M urea at 60°C.

coming from human or animal, which is very common and huge. Direct urine fuel cell can possibly be applied to purify urine through urea oxidation reaction with electricity generated at the same time, especially in manned spaceship and submarine as a part of life support system. Further related researches such as urine-tolerant separator and reaction mechanisms need to be carried out to make it an alternative to produce electricity or even treat wastewater.

Methods

Preparation of NiCo/C catalysts and electrodes. Nickel-cobalt catalysts were prepared by the $NaBH_4$ reduction method. Typically, $NiSO_4 \cdot 6H_2O$, $CoCl_2 \cdot 6H_2O$ and citric acid were dissolved into 250 mL deionized water in a flask with specific weight ratio. The solution was treated by 15 minutes aeration of nitrogen gas. Then fresh $NaBH_4$ solution (4 wt%) was added dropwise into the mixed aqueous solution with violently stirring. After stirring for 3 hours, black carbon (Carbon Vulcan XC-72R) was added into the bottle. Three hours later, the mixture was filtered and washed with deionised water for 3–5 times. The precipitate was dried in vacuum oven at 50°C overnight. Five kinds of catalysts were prepared with Co contents of 0, 10, 20, 30, 40 wt% respectively, and the carbon weight percent was 50% in all catalyst. Accordingly we call them Ni/C, Ni_4Co_1/C, Ni_3Co_2/C, Ni_2Co_3/C and Ni_1Co_4/C respectively.

Carbon cloth (Hesen, Shanghai, China) was immersed in 30% PTFE solution (Hesen, Shanghai, China) for 10 min, and then heated at 370°C for 25 min as pre-treatment. Catalysts were mixed with isopropanol, water and 5% Nafion (DE520, DuPont, USA) in ultrasonic bath for 30 minutes to obtain catalyst inks. They were coated on the carbon cloth using a paintbrush with the NiCo loading of ~10 mg cm^{-2}. Then the electrodes coated catalysts were dried in air for at least 24 h prior to use. The geometric area of all electrodes was 2.0 cm^2. Pt/C coated carbon cloth was used as cathode with a Pt loading of ~1.0 mg cm^{-2}.

Characterizations of catalysts. X-ray diffraction (XRD) measurements were performed by using Shimadzu XRD-6000 equipped with a Cu-Kα radiation source ($\lambda = 1.54056$ Å) and operating at 40 kV and 40 mA. The data of XRD between 15° and 85° 2θ angular regions was collected.

Surface composition of the bimetal catalyst was inferred from X-ray photoelectron spectroscopy (XPS), using an ESCALAB_250Xi X-ray photoelectron spectrometer

with Al Kα X-ray as the excitation source. The sample was pressed to an 8 mm diameter disc before test. The charging effect of the sample was corrected by standard carbon (C1s = 284.6 eV).

The obtained Ni/C and NiCo/C electrocatalysts were characterized by transmission electron microscopy (TEM, JEOL JEM-1230) at a voltage of 120 kv. The sample was dispersed in alcohol solvent by ultrasonic action and dropped onto a carbon-coated copper grid. Scanning Electron Microscopes (SEM) were conducted by Hitachi TM1000.

Electrochemical measurements were conducted in 1 M KOH or 0.33 M urea +1 M KOH using glass carbon electrode (GCE) with 3 mm diameter connected to an electrochemical workstation (CHI 660D, Shanghai Chenhua). Typically, 5 mg catalyst was mixed with 0.1 mL Nafion and 0.4 mL water in ultrasonic bath for 30 minutes to get catalyst ink. Then 6 μL of ink was dropped onto GCE (3 mm diameter) and dry at room temperature. A platinum foil (0.3 cm^2) was used as the counter electrode. An Hg/HgO electrode (MMO) was used as reference electrode. The electrolyte was bubbled by nitrogen gas for 20 minutes before the tests. Cyclic voltammograms (CV) were performed from 0.2 V to 0.8 V *vs.* MMO at a scan rate of 50 mV s^{-1}, and all results were collected after scanning at least for 5 times.

Electrical conductivities (σ) were measured at room temperature by a digital four-probe measuring instrument (RTS-8, 4 PROBES TECH, CHINA) controlled by a computer. The catalysts were compressed into sheets before measurement.

Fuel cell testing and analysis. Anion exchange membrane (AEM, AMI-7001, AMFOR INC.) is used as polymer electrolyte to make membrane electrode assembly (MEA)[3,4], both the anode and cathode have the same active area of 2.0 × 2.0 cm. Stainless steel plates with serpentine flow channels are used as the flow field plates and current collectors both at the cathode and anode. At the anodes, 0.33 M urea or urine is fed into flow channel as fuels at a flow rate of 3.0 mL min^{-1} by peristaltic pumps, and they are kept in a constant temperature water bath. At the cathodes, humidification oxygen is used as electrons acceptor. A data acquisition system (PISO-813, ICP DAS) is used to measure the fuel cell performance. RP-HPLC (FL2200) was applied to the determination of urea in human urine separating by Waters Atlantis T3. The concentration of urea was determined by diode array detector at the wavelength of 195 nm.

1. Meessen, J. H. [Urea]. *Ullmann's Encyclopedia of Industrial Chemistry.* (Wiley-VCH, Germany, 2010).

2. Shriver, D. & Atkins, P. *Inorganic Chemistry*. (W. H. Freeman, the United States, 2010).
3. Lan, R. & Tao, S. Preparation of nano-sized nickel as anode catalyst for direct urea and urine fuel cells. *J. Power Sources* **196**, 5021–5026 (2011).
4. Lan, R., Tao, S. & Irvine, J. T. S. A direct urea fuel cell - power from fertiliser and waste. *Energy Environ. Sci.* **3**, 438–441 (2010).
5. Hamonts, K. *et al.* Influence of soil bulk density and matric potential on microbial dynamics, inorganic N transformations, N_2O and N_2 fluxes following urea deposition. *Soil Biol. Biochem.* **65**, 1–11 (2013).
6. Chang, J. J., Wu, S. Q., Dai, Y. R., Liang, W. & Wu, Z. B. Nitrogen removal from nitrate-laden wastewater by integrated vertical-flow constructed wetland systems. *Ecol. Eng.* **58**, 192–201 (2013).
7. Choi, I. D., Lee, H., Shim, Y. B. & Lee, D. A one-Step continuous synthesis of carbon-supported Pt catalysts using a flame for the preparation of the fuel electrode. *Langmuir* **26**, 11212–11216 (2010).
8. Dutta, A. & Datta, J. Outstanding catalyst performance of PdAuNi nanoparticles for the anodic reaction in an alkaline direct ethanol (with anion-exchange membrane) fuel cell. *J. Phys. Chem. C* **116**, 25677–25688 (2012).
9. Fu, Q. *et al.* Interface-confined ferrous centers for catalytic oxidation. *Science* **328**, 1141–1144 (2010).
10. Sun, S. *et al.* Single-atom catalysis using Pt/graphene achieved through atomic layer deposition. *Sci. Rep.* **3**, 1775 (2013).
11. Hwang, S. J. *et al.* Supported core@shell electrocatalysts for fuel cells: close encounter withreality. *Sci. Rep.* **3**, 1309 (2013).
12. Boggs, B. K., King, R. L. & Botte, G. G. Urea electrolysis: direct hydrogen production from urine. *Chem. Commun.* **32**, 4859–4861 (2009).
13. King, R. L. & Botte, G. G. Hydrogen production via urea electrolysis using a gel electrolyte. *J. Power Sources* **196**, 2773–2778 (2011).
14. Tang, Y. *et al.* Electro-catalytic performance of PdCo bimetallic hollow nano-spheres for the oxidation of formic acid. *J. Solid State Electrochem.* **14**, 2077–2082 (2010).
15. Wang, X. & Xia, Y. Electrocatalytic performance of PdCo–C catalyst for formic acid oxidation. *Electrochem Commun.* **10**, 1644–1646 (2008).
16. Huang, H., Fan, Y. & Wang, X. Low-defect multi-walled carbon nanotubes supported PtCo alloy nanoparticles with remarkable performance for electrooxidation of methanol. *Electrochim. Acta* **80**, 118–125 (2012).
17. Wang, Z. *et al.* High electrocatalytic activity of non-noble Ni-Co/graphene catalyst for direct ethanol fuel cells. *J. Solid State Electrochem.* **17**, 99–107 (2013).
18. Vidotti, M. *et al.* Electrocatalytic oxidation of urea by nanostructured nickel/cobalt hydroxide electrodes. *Electrochim. Acta* **53**, 4030–4034 (2008).
19. Yan, W., Wang, D. & Botte, G. G. Nickel and cobalt bimetallic hydroxide catalysts for urea electro-oxidation. *Electrochim. Acta* **61**, 25–30 (2012).
20. Ding, R. *et al.* Facile synthesis of mesoporous spinel $NiCo_2O_4$ nanostructures as highly efficient electrocatalysts for urea electro-oxidation. *Nanoscale* **6**, 1369–1376 (2014).
21. Hernandez-Fernandez, P. *et al.* Effect of Co in the efficiency of the methanol electrooxidation reaction on carbon supported Pt. *J. Power Sources* **195**, 7959–7967 (2010).
22. Gojkovic, S. L. Electrochemical oxidation of methanol on Pt3Co bulk alloy. *J. Serb. Chem. Soc.* **68**, 859–870 (2003).
23. Salgado, J. R. C., Antolini, E. & Gonzalez, E. R. Carbon supported Pt–Co alloys as methanol-resistant oxygen-reduction electrocatalysts for direct methanol fuel cells. *Appl. Catal. B* **57**, 283–290 (2005).
24. Putnam, D. F. *Composition and Concentrative Properties of Human Urine*. (NASA Contractor Report, the United States, 1971).
25. Dai, W.-L., Qiao, M.-H. & Deng, J.-F. XPS studies on a novel amorphous Ni–Co–W–B alloy powder. *Appl. Surf. Sci.* **120**, 119–124 (1997).
26. Biesinger, M. C., Payne, B. P., Grosvenor, A. P., Lau, L. W. M., Gerson, A. R. & Smart, R. St. C. Resolving surface chemical states in XPS analysis of first row transition metals, oxides and hydroxides: Cr, Mn, Fe, Co and Ni. *Appl. Surf. Sci.* **257**, 2717–2730 (2011).
27. Vidotti, M., Silva, M. R., Salvador, R. P., Córdoba de Torresi, S. I. & Dall'Antonia, L. H. Electrocatalytic oxidation of urea by nanostructured nickel/cobalt hydroxide electrodes. *Electrochim. Acta* **53**, 4030–4034 (2008).
28. Kim, J. W. & Park, S. M. In situ XANES studies of electrodeposited nickel oxide films with metal additives for the electro-oxidation of ethanol. *J. Electrochem. Soc.* **150**, E560–E566 (2003).
29. Córdoba de Torresi, S. I., Provazi, K., Malta, M. & Torresi, R. M. Effect of additives in the stabilization of the α Phase of $Ni(OH)_2$ electrodes. *J. Electrochem. Soc.* **148**, A1179–A1184 (2001).
30. Armstrong, R. D. & Charles, E. A. Some effects of cobalt hydroxide upon the electrochemical behaviour of nickel hydroxide electrodes. *J. Power Sources* **25**, 89–97 (1989).
31. Armstrong, R. D., Briggs, G. W. D. & Charles, E. A. Some effects of the addition of cobalt to the nickel hydroxide electrode. *J. Appl. Electrochem.* **18**, 215–219 (1988).

Acknowledgments

Author contributions

W.X. proposed the concept. Z.W. directed the research. W.X., H.Z. and Z.W. designed the experiments. W.X., H.Z. and G.L. carried out the experiments. W.X. and H.Z. wrote the main manuscript text and prepared figures. All authors reviewed the manuscript.

Additional information

Competing financial interests: The authors declare no competing financial interests.

How to cite this article: Xu, W., Zhang, H., Li, G. & Wu, Z. Nickel-cobalt bimetallic anode catalysts for direct urea fuel cell. *Sci. Rep.* **4**, 5863; DOI:10.1038/srep05863 (2014).